Available online at www.sciencedirect.com
ScienceDirect
Ceramics International 33 (2007) 1557–1561
CERAMICS INTERNATIONAL
www.elsevier.com/locate/ceramint

Sinterability, crystallization and properties of glass–ceramic tiles belonging to CaF_2–CaO–MgO–Al_2O_3–SiO_2 system

S. Banijamali, H.R. Rezaei, B. Eftekhari Yekta *, V.K. Marghussian

Materials Department, Iran University of Science and Technology, Tehran, Iran

Received 16 September 2005; received in revised form 1 April 2006; accepted 28 June 2006
Available online 14 September 2006

Abstract

The effect of CaO substitution by different amounts of MgO on crystallization and various properties of CaF_2–CaO–Al_2O_3–SiO_2 glass system were investigated. It was shown that the properties of obtained glass–ceramics are greatly influenced by MgO contents. The Avrami exponent and activation energy for crystallization of the most promising and the MgO-free specimens were determined. Results suggested that surface crystallization was the main precipitation mechanism of both samples and while the activation energy for crystallization of MgO containing sample was less than MgO-free one, its ability to crystallize was diminished. SEM results confirm occurrence of surface crystallization of samples and depicts the phenomenon of microstructure coarsening by increasing MgO content and also reduced densification of specimen with magnesium oxide more than 9 wt.%.

Keywords: D. Glass–ceramics; Sinterability; Calcium fluoride; Calcium aluminum silicate glasses

1. Introduction

Sintering of glass powders is an efficient technique to obtain glass–ceramic materials. In this technique sintering and crystallization can occur in a single stage heat treatment [1,2]. A completely dense and crystallized body is obtained when densification occurs before it is halted by crystallization. In fact when crystallization starts, glass viscosity is increased and delays sintering by reduction of specimen fluidity [3–5]. Therefore, densification tendency in specimen in which bulk crystallization takes place, is considerably lower than a glass in which surface crystallization is dominant [6,7].

Recently, most researches on ceramic floor tile composition have been focused on glass–ceramic bodies. These products are able to satisfy the requirements of chemical and abrasion resistance, good mechanical strength and attractive appearance [1]. Sintered glass–ceramics in CaO–Al_2O_3–SiO_2 system are good candidates for tile applications. High hardness, scratching and chemical resistance beside the availability and low cost raw materials make this system a wise choice [1,8].

In a previous study [9], the effects of fluorine on sinterability and crystallization of a CAS glass composition were investigated. It was found that addition of 9 weight parts fluorine, gives the best assembly of chemical and mechanical properties. In the present work we have tried to study the effects of CaO substitution by MgO, in order to improve the mechanical and chemical properties of the previous CAS glass–ceramic.

2. Experimental procedure

Table 1 shows the chemical composition of glasses. The glass batches were prepared from commercial grades dolomite (Setabran), $CaCO_3$ (Azna), α-Al_2O_3 (Fibrona), silica (Setabran) and fluorine (Tabas). The mixtures of raw materials were transferred to a zircon crucible and melted at 1450 °C for 1 h in an electric furnace. Then melts were water quenched and the resulting frits were dried and milled to the required size (<75 μm). Particle size distributions of glass powders were characterized by a laser particle size analyzer (Fritsch analysete 22).

Glass powders with 0.2 wt.% carboxy methyl cellulose (CMC) water solution (based on dried frit weight) were uniaxually pressed at 30 MPa and were shaped in a 20 mm

* Corresponding author.
E-mail address: beftekhari@iust.ac.ir (B. Eftekhari Yekta).

0272-8842/$32.00
doi:10.1016/j.ceramint.2006.06.004

Table 1
Chemical composition of glasses (weight part)

Glass composition	SiO_2	Al_2O_3	CaO	MgO	CaF_2
SF9	33.63	42.84	23.54	–	9
SF9M3	33.63	42.84	20.54	3	9
SF9M6	33.63	42.84	17.54	6	9
SF9M9	33.63	42.84	14.54	9	9

cylindrical die. The obtained compacts were then sintered in an electric laboratory furnace at temperatures from 850 to 1050 °C. For firing the samples a constant heating rate of 7 °C/min and a soaking time of 1 h were used and then the furnace was allowed to cool down. Linear shrinkage and water absorption (according to EN 99 standard) were measured to evaluate sintering behavior. The thermal behavior of the glasses was monitored by differential thermal analysis (Netzsch 404) using a heating rate of 10 °C/min in air. Alumina was used as the reference material.

Crystalline phases precipitated in the sintered samples were identified using X-ray diffractometers (Siemens-D500, Jeol JDX-8030). Bending strength was measured using three point bending method according to C158 ASTM in MTS machine (10/M) at a cross-head speed of 0.6 mm min^{-1}. The average value was obtained from measurement of five samples. The microhardness of the glass–ceramics was measured using a Vickers tester (Buehler, Micromete1) on polished samples with an indentation of 100 gf for 30 s. The average value was obtained from 10 indentations. The chemical resistance of the glass–ceramics was examined according to a modified EN106 standard, in which chemical resistance was determined as the weight difference of specimens, before and after chemical leaching.

The microstructures of the sintered samples were evaluated by scanning electron microscope (Phillips XL30) after polishing and etching in 5% HF solution for 15 s.

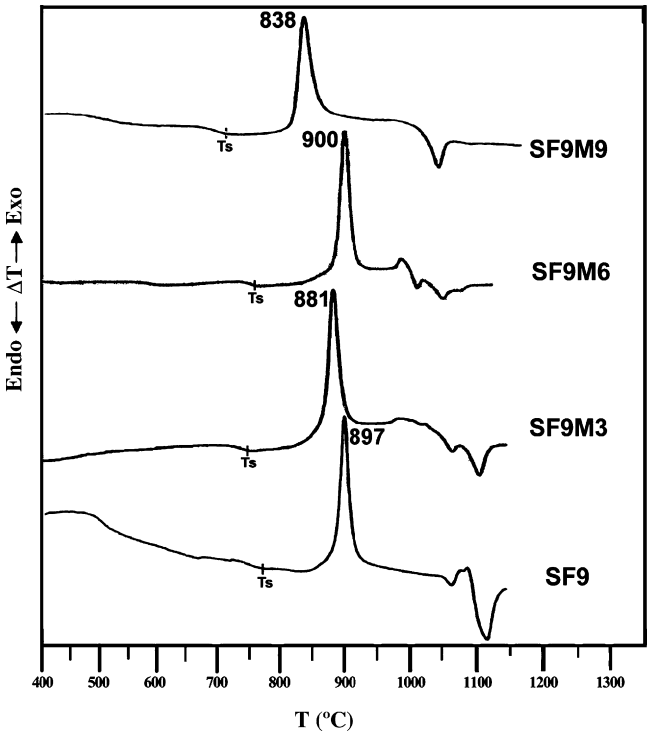

Fig. 1. DTA profiles of samples (<75 μm) at a heating rate of 10 °C/min.

3. Results and discussion

Fig. 1 shows the DTA profiles of glasses containing different amounts of MgO and MgO-free glass (SF9). It can be seen that gradual substitution of CaO by MgO in the base glass (SF9) leads to decrease in dilatometric softening point (T_s) and crystallization peak temperatures (T_p) and also changes of endothermic peak shape and its intensity. It seems that although Mg^{2+} ion has a greater ionic field strength than Ca^{2+} ion,

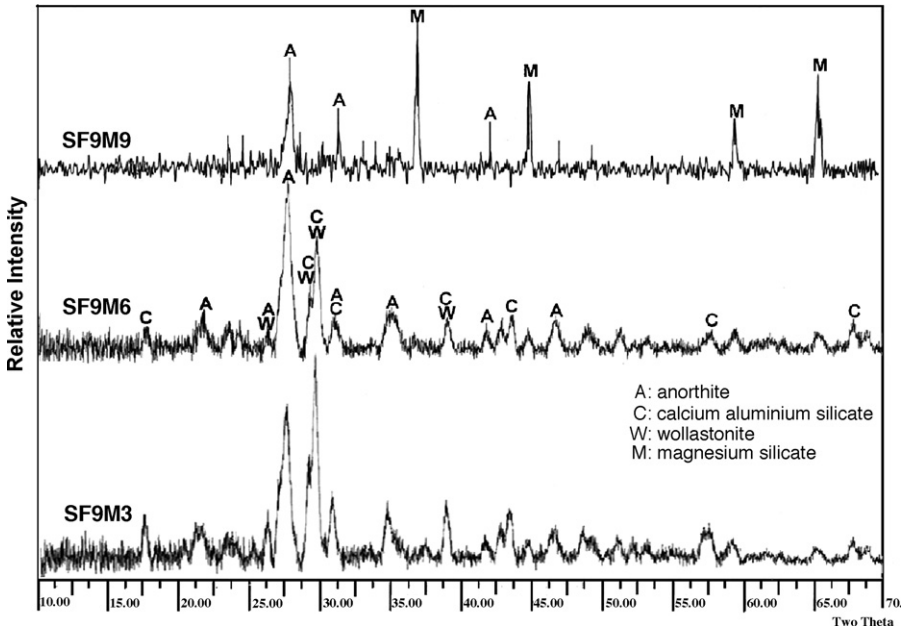

Fig. 2. XRD patterns of sintered samples at the crystallization peak temperature for 1 h.

however its smaller size and higher mobility cause the mentioned effect appears with addition of MgO to the glass. It should also be noted that the viscosity of glasses can be reduced by making them more complex, probably through making new eutectic temperatures [10].

Fig. 2 shows the X-ray diffraction patterns of fired compacted glass powders at their main DTA crystallization peak temperature for 1 h. As it can be seen similar crystalline phases, wollastonite ($CaO{\cdot}SiO_2$), calcium aluminum silicate ($CaO{\cdot}Al_2O_3{\cdot}SiO_2$) and anorthite ($CaO{\cdot}Al_2O_3{\cdot}2SiO_2$) exist in SF9M3 and SF9M6. In SF9M6, a lower CaO content leads to intensification of anorthite and degradation of two other phases. Since in these two samples the same kinds of crystalline phases are precipitated at T_p, increasing of MgO content in SF9M6 should lead to enlargement of diffusion path between their components and so decreases the ability to crystallize.

It can also be seen that in glasses SF9M3 and SF9M6 a second weak exothermic peak appears at about 1000 °C, too. X-ray diffraction analysis indicated that this peak is related to the crystallization of magnesium silicate ($MgO{\cdot}SiO_2$) which shifted to a lower temperature (838 °C), with increasing MgO, as a main crystallization peak in glass SF9M9. Furthermore, in each MgO bearing glass a new endothermic peak can be observed (above 1000 °C) which is related to the melting of a crystalline phase and/or liquidus temperature.

To study sinterability behavior of MgO bearing glass powders ($T_s - T_p$), temperature interval was extracted from related DTA profiles and determined for each sample. Since viscous flow occurs after T_s, widening of this interval delays crystallization, so that sintering happens more effectively before it is stopped by crystallization [4,6]. This parameter was found to be 145°, 175° and 126 °C for SF9M3, SF9M6 and SF9M9 glass–ceramics, respectively. Good densification of SF9M3 and SF9M6 (at about 950 °C) and weak sinterability of SF9M9 are almost in agreement with this idea. Noticeable precipitation of a high density magnesium silicate phase (~4 g/cm^3) can introduce some porosity into the system during densification and thus may prevent complete densification, too.

Fig. 3 shows the X-ray diffraction patterns of the MgO bearing glasses and the MgO-free one (SF9) after sintering at their optimum sintering temperature. Phase evaluation of the MgO containing glass powders during sintering showed that sintering of SF9M3, SF9M6 and SF9 bodies up to 1000 °C leads to crystallization of similar phases. With increasing temperature, beside previous phases the patterns of magnesium silicate appear with their intensities being sharper in SF9M6 than SF9M3. At 1050 °C, the intensity of wollastonite and calcium aluminum silicate peaks is degraded. Since this temperature is near to the first endothermic peak, it seems that the mentioned phases are beginning to dissolve in the glass matrix at this temperature. Contrary to our initial expectation, none of the other modifications of magnesium aluminosilicate phases, e.g. diopside ($CaO{\cdot}MgO{\cdot}2SiO_2$), were precipitated in the MgO containing glass–ceramics. It was due to lack of known suitable nucleating agents, e.g. Fe_2O_3, Cr_2O_3 and TiO_2 in the glass compositions where their presence could cause undesirable colors in the specimens. By increasing MgO and

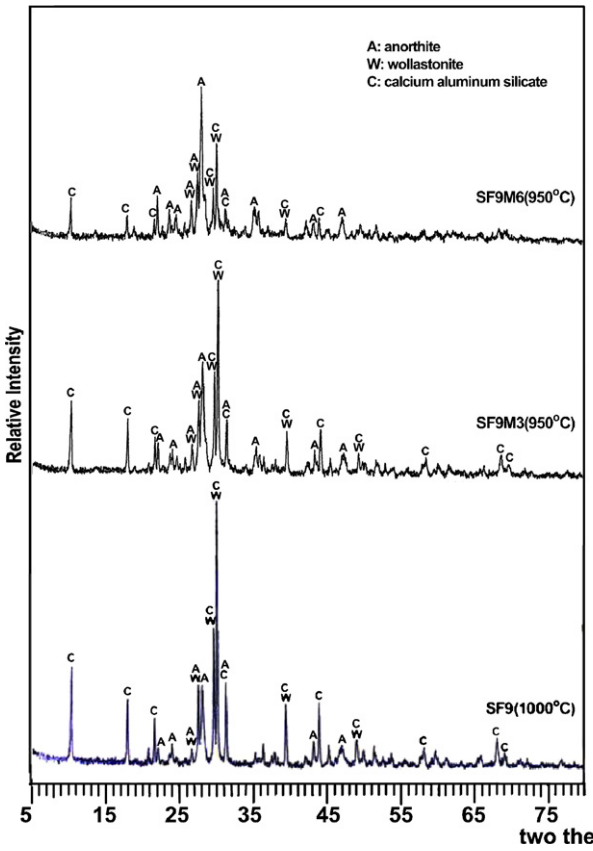

Fig. 3. XRD patterns of densified SF9, SF9M3 and SF9M6 at their optimum sintering temperature.

subsequently decreasing glass viscosity, enhancement in crystallinity is expected [11–13]. However, comparison of relative intensity of crystalline phases by XRD patterns shows an opposite trend. This effect is particularly related to the reduction in concentration of calcium ion which reduces ability of the system to crystallize calcium bearing phases.

Table 2 shows the results of mechanical and chemical measurements of SF9, SF9M3 and SF9M6 glass–ceramics after sintering at their optimum temperatures. It can be seen that while substitution of CaO by MgO and increasing MgO content of glass improves Vickers microhardness and chemical resistance, it does degrade bending strength. This degradation is related to the reduction in crystallinity. As in the MgO bearing glasses, MgO did not enter into the crystalline phases before 1000 °C and remained in the residual glass matrix, increased its hardness. On the other hand by increasing MgO content, the quantity of harder anorthite phase [14] was increased. This trend was also observed for chemical resistance which means stronger glass structural bonds in residual glassy

Table 2
Mechanical and chemical properties of sintered glass–ceramics

Properties	SF9	SF9M3	SF9M6
Bending strength (MPa)	123.15	103.95	67.18
Vickers hardness (GPa)	5.64	6.13	6.65
Weight loss (%)	2.20	1.14	0.86

Table 3
The values of the activation energy for crystallization and parameter n related to mechanism of crystallization

Specimen	E (Augis-Bennett) (kJ/mol)	E (modified Kissinger) (kJ/mol)	E (Marotta) (kJ/mol)	n (Marotta)	n (Ozawa)
SF9	612.49	642.1	625.7	0.89	1.32
SF9M6	398.6	386	411.7	0.86	1.07

phase improve chemical resistance. Furthermore, it can be said that by increasing MgO in glass, the crystallinity is decreased which is accompanied with reduction in the glass–crystal interfaces so chemical resistance is improved [15].

Among studied glass–ceramics, sample SF9M6 is the most promising one in point of microhardness and chemical resistance view. So to obtain a better understanding of crystallization mechanism and the role of Mg^{2+} ion on it, the activation energy for crystallization and the Avrami exponent of SF9 and SF9M6 were determined. To determine these parameters each sample was examined at different heating rate of 5, 10, 15 and 20 °C/min by DTA method.

Table 3 shows the calculated activation energy for crystallization and Avrami exponent of glasses. Near unity Avrami exponent confirms surface crystallization of both samples. It should be pointed out that although the results show lower activation energy for crystallization of glass SF9M6, XRD patterns (Fig. 3) indicate a lowered crystallinity for it. To understand this complication, the Gibbs free energy changes during crystallization (ΔG) was considered according to Eq. (1) [1]:

$$\Delta G = -(4/3)\pi r^3 \Delta G_V + 4\pi r^2 \gamma \quad (1)$$

where here γ, r and ΔG_V are the glass–crystal interface surface energy, nuclei radius and the bulk free energy change due to liquid-to-crystal transformation (per mole), respectively. ΔG_V in turn can be calculated according to Eq. (2) [1]:

$$\Delta G_V = \frac{L\Delta T}{T_m} \quad (2)$$

where here L, T_m and ΔT represent the heat of fusion per mole, melting temperature and undercooling amount (interval temperature of liquidus and crystallization peak), respectively. With assumption of a constant L for both glasses, the $\Delta G_{V(SF9)}/\Delta G_{V(SF9M6)}$ ratio, extracted by fitting the results of DTA runs (Fig. 1) into Eq. (2), was 1.15. Thus it can be said that sample SF9 attains a greater thermodynamic driving force for

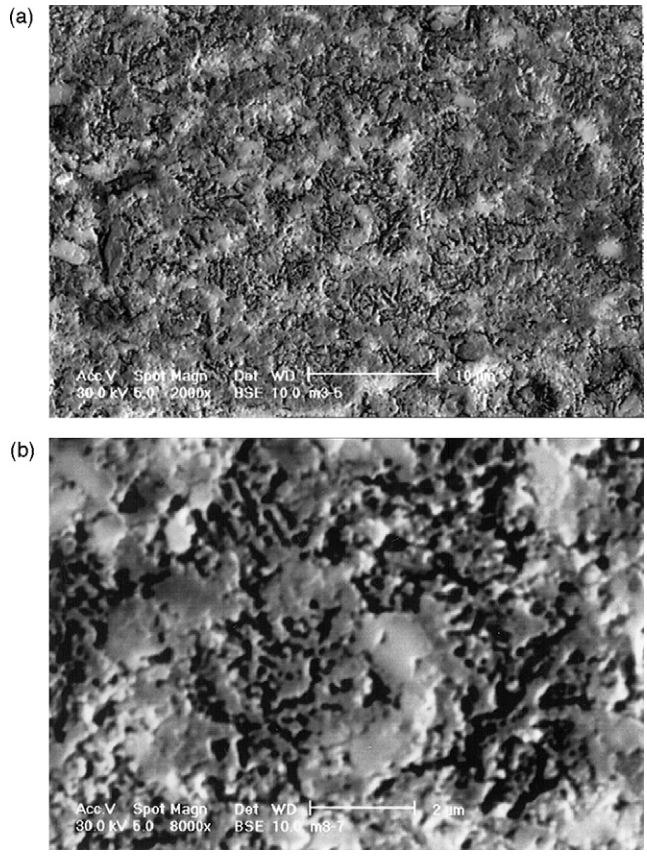

Fig. 4. SEM micrographs of sample SF9M3 sintered at 1050 °C for 1 h: (a) 2000× and (b) 8000×.

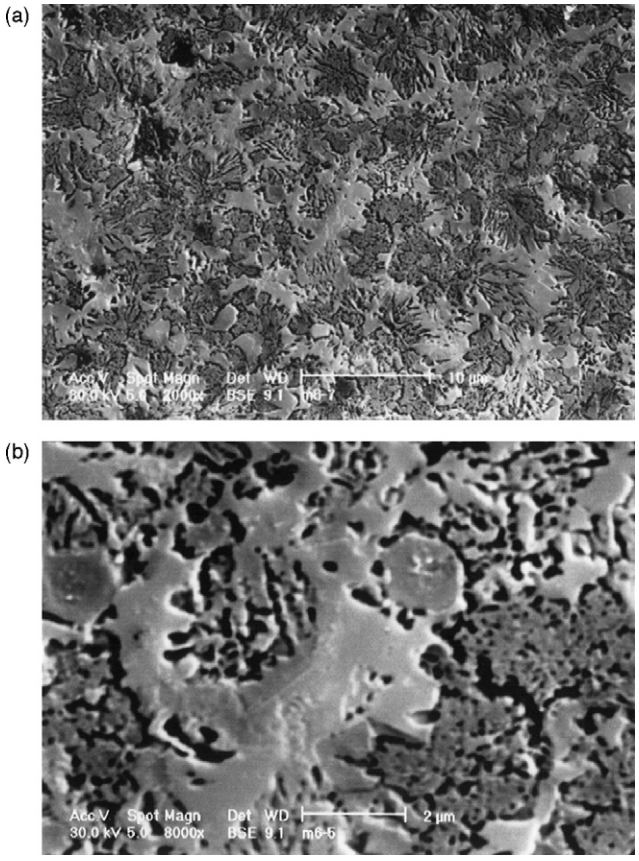

Fig. 5. SEM micrographs of sample SF9M6 sintered at 1050 °C for 1 h: (a) 2000× and (b) 8000×.

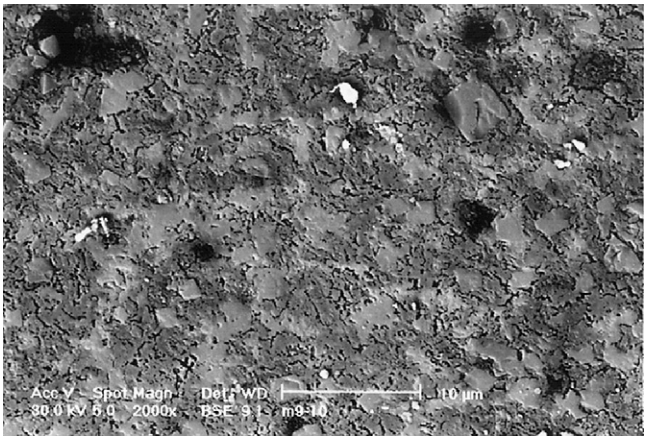

Fig. 6. SEM micrograph of sample SF9M9 sintered at 1050 °C for 1 h.

crystallization rather than sample SF9M6. On the other hand, γ (another thermodynamic parameter) tends to be lower the closer the compositions of the initial glass and the precipitating phase [16]. Therefore, since the same crystalline phases precipitated near to crystallization temperature of both glasses, SF9M6 is expected to have a greater surface energy. Thus despite its lower activation energy, this glass was crystallized less than SF9, due to the lower thermodynamic driving force and greater surface energy. The extracted activation energies for crystallization of glasses are not in agreement with obtained values by other researchers and are considerably higher. Maybe it is related to the composition differences and also using finer powders by them [7].

Figs. 4–6 show the microstructure of sintered glass–ceramics. Obviously all specimens are crystallized from free surfaces of their compacted particles. A comparison between Figs. 4 and 5 represents also a coarser microstructure of SF9M6 rather than of the SF9M3, probably due to the higher crystallization temperature and lower concentration of constituent ions. It seems microstructure coarsening and low crystallinity are responsible for lower bending strength of SF9M6. SF9M9 had a similar microstructure to the other specimens, however it contained more porosity, due to its poorer sinterability.

4. Conclusion

1. Dependent on the MgO content, CaO substitution by MgO has different effects on sintering and crystallization behavior. Using MgO up to 6 wt.% improves sinterability via decreasing viscosity and crystallinity, while still higher MgO contents suppress the sinterability trend.
2. Since surface hardness and chemical resistance are essential factors for floor tiles applications, sample SF9M6 is the most promising specimen. Presence of harder residual glass phase and considerable anorthite are responsible for this improved performance.
3. Calculated activation energy for crystallization and the Avrami exponent of glasses SF9 and SF9M6 suggest surface crystallization of both samples and a lower activation energy for crystallization of SF9M6, however this sample achieves lower crystallinity because of its lower thermodynamic driving force for crystallization.
4. While increasing MgO content decreases bending strength, it improves the chemical resistance. It seems this behavior is related to lower crystallinity and also stronger residual glassy phase which is attained by substitution.

References

[1] W. Holland, G. Beall, Glass–Ceramic Technology, American Ceramic Society, Ohio, 2002.
[2] Z. Strnad, Glass–Ceramic Materials: Glass science and Technology, Elsevier, New York, 1986.
[3] C. Siligardi, M.C. D'Arrigo, C. Leonelli, Sintering behavior of glass–ceramics frits, Am. Ceram. Soc. Bull. 79 (2000) 88–92.
[4] M. Aloisi, A. Karamanov, M. Pelino, Sintered glass–ceramics from municipal waste incinerator ashes, J. Non-Cryst. Solids 345 (2004) 192–196.
[5] A. Karamanov, M. Aloisi, M. Pelino, Sintering behavior of a glass obtained from MSWI ash, J. Eur. Ceram. Soc. 25 (2005) 1531–1540.
[6] E.M. Rabinovich, Review: preparation of glass by sintering, J. Mater. Sci. 20 (1985) 4259–4297.
[7] K. Sujirote, R.D. Rawlings, P.S. Rogers, Effect of fluoride on sinterability of a silicate glass powder, J. Eur. Ceram. Soc. 18 (1998) 1325–1330.
[8] C. Lira, A.P. Oliveira, O.E. Alarcon, Sintering and crystallization of CaO–Al_2O_3–SiO_2 glass powder compacts, Glass Technol. 42 (2001) 91–96.
[9] S. Banijamali, B. Eftekhari Yekta, H.R. Rezaei, V.K. Marghussian, Effect of fluorine on the sintering and crystallization behavior of CaO–Al_2O_3–SiO_2 glass–ceramic system, Adv. Appl. Ceram., in press.
[10] M.B. Volf, Technical Approach to Glass, Glass Science and Technology, Elsevier, 1990.
[11] P. Rocaboise, J.N. Pontoire, J. Lehmann, H. Gaye, Crystallization of CaO–Al_2O_3–SiO_2 based oxide inclusions, J. Non-Cryst. Solids 282 (2001) 98–109.
[12] T. Toya, Y. Tamura, Y. Kameshima, K. Okada, Preparation and properties of CaO–MgO–Al_2O_3–SiO_2 glass–ceramics from kaolin clay refining waste (Kira) and dolomite, Ceram. Int. 30 (2004) 983–989.
[13] V.K. Marghussian, M.H. Dayi Niaki, Effects of composition changes on the crystallization behavior and properties of SiO_2–Al_2O_3–CaO–MgO(-Fe_2O_3–Na_2O–K_2O) glass–ceramics, J. Eur. Ceram. Soc. 15 (1995) 343–348.
[14] M. Kuzin, N. Egorove, Field Manual of Minerals, Mir Publishers, Moscow, 1976.
[15] B. Eftekhari Yekta, B. Tabatabaei, S. Hashemi Nia, Preparation of acid-resistance glass and glass–ceramics using copper slag, Ind. Ceram. 24 (2004) 115–120.
[16] P.F. James, Nucleation in Glass-forming Systems: A Review, Nucleation and Crystallization in Glasses, American Ceramic Society, Ohio, 1981.